Comparing Threshold Based Denoising Methods in Wavelet Transform Domain

A. Mohammad Zaki, and S. Ghofrani*
Electrical Engineering Department,
South Tehran Branch, Islamic Azad University, Tehran, Iran.
Email: alirezamzaki@gmail.com, s_ghofrani@azad.ac.ir

***Abstract*—**In this paper, the principal concept of image denoising in wavelet domain is discussed. For this purpose, three thresholding approaches known as VisuShrink, SureShrink and NeighBlock are employed, three noise power estimators named Median absolute deviation, Quantile median and Marginal variance are used and four thresholding rules called hard, soft, Exp. and Garrot are applied. All methods take effort for denoising in transform domain. As a matter of fact, sparsity of coefficients, in addition to the noise power estimator efficiency, are the key roles for every thresholding method. So, we focus on the capability for noise power estimation to discover the most optimal method for image denoising in wavelet domain. Being consistent in estimating the noise power in every wavelet decomposition level, it was believed that Median absolute deviation was the best method. To challenge this idea, outcome of mentioned method and other noise power estimators is to be compared. Finally, some packages will be proposed that each of them introduce methods and algorithms that act together optimally. The performance evaluation is via two points of view, Speckle noise reduction and image quality preservation. The most optimal package which outperforms others is using Garrot thresholding rule and Median absolute deviation in VisuSrink denoising method.

***Keywords*—**Wavelet transform, Noise power estimation, Thresholding, Denoising.

I. Introduction

Real world data rarely comes clean or noise-free though the noise might be negligible under high signal to noise ratio (SNR). Having destructive effects, many models such as Gaussian [1], speckle [2] and poisson [3] were proposed for noise identification. The term "signal denoising" is general but it is usually devoted to the recovery of a signal that has been contaminated by additive white Gaussian noise (AWGN) rather than other types (eg. non-additive, poisson and speckle).

Due to overcoming the noise draw backs, many approaches either in spatial domain [4] or frequency domain [5], were proposed. Median and Wiener filters [6]-[10] are two popular method in signal domain but fail to preserve the image details. In frequency domain, wavelet transform is widely used for data denoising. According to the fact that it simplifies signal statistics, the wavelet transform is so popular between all transforms.

As a general rule, wavelet threshold based denoising techniques perform well in presence of additive noise [11]-[14]. The orthogonality of discrete wavelet transform (DWT) leads to the feature that the white noise transformed into white noise [11]-[14] which means spreading. For each decomposition level ℓ, the DWT produces four wavelet sub-images: $A_\ell, h_\ell, v_\ell, d_\ell$, where A_ℓ is the approximation or coarse coefficient and h_ℓ, v_ℓ, d_ℓ are the horizontal, vertical, diagonal details coefficients.

It is known that one important characteristic of noise is adding high-frequency components to the original signal. As approximation coefficients (A_ℓ) represent "low-frequency" terms, they are less affected by noise. Hence, thresholding methods are usually applied to the detail coefficients.

Two properties of the discrete wavelet transform are:

1. Sparsity, that means a few large coefficients dominate the representation.
2. Decorrelation, that means the coefficients tend to be much less correlated than the original data.

So, the wavelet coefficients can be processed independently (decorrelation property) and small valued coefficients are removed (sparsity) [15].

There are several nonlinear thresholding methods [15], [16] which are used in transform domain. In general, all wavelet based thresholding methods replace noisy coefficients with zeros according to a fixed value as the threshold, and keeping the others. The performance of this nonlinear process known as wavelet shrinkage depends on the threshold value [5], [17]. So, the noise power $\hat{\sigma}_n$ in each decomposition level should be estimated at first [18], [19], then the threshold value λ obtained.

In this paper the performance of three popular denoising algorithms named VisuShrink, SureShrink and NeighBlock are compared according to visual evaluation as well as three image assessment parameters. In this regard, Median absolute deviation, Quantile median, Marginal variance are used for noise power estimation and hard, soft, Exp., Garrot are applied as thresholding rules.

The organization of this paper is as follows. Section 2 briefly explains the thresholding theory, thresholding rules, noise power estimators and threshold-based denoising algorithms in any transform domain such as DWT. Section 3 shows the experimental results belong to three well known

Alireza Mohammad Zaki was with Islamic Azad University, South Tehran Branch (e-mail: alirezamzaki@gmail.com).

Sedigheh Ghofrani is the associate professor of Islamic Azad University, South Tehran Branch, Tehran, Iran. (Corresponding author to provide phone: +98-21-88731446, Fax: +98-21-88532683; e-mail: s_ghofrani@azad.ac.ir).

methods under employing various noise power estimators and different thresholding rules. Finally, Section 4 is dedicated to conclusion and discussion.

II. WAWELET THRESHOLDING

The wavelet based thresholding methods involve three steps: 1. Computing the forward transform coefficients of noisy image, 2. Filtering the coefficients by means of a thresholding process, 3. Using the inverse transform to retrieve the denoised image, see Fig. 1.

A. Problem Formulation

It is proved that speckle which degrades any images of coherent systems like ultrasound and radar can be modeled as a multiplicative noise [2], [20], [21],

$$I = I_r \times E \tag{1}$$

where I and I_r are the noisy and noise free images and E is the noise component having real and imaginary parts independent, zero mean and identically distributed [2], [20]. In order to convert the multiplicative noise model into additive, the homomorphic framework processing which means applying the algorithm function at first and exponential function at the end is used. Hence, the additive noise can be assumed approximately Gaussian [22]-[25].

$$Y = F + N \tag{2}$$

where $Y = \log I$ is the noisy data, $F = \log I_r$ is the clean or noise free data and $N = \log E$ is AWGN. For every decomposition level ℓ, the wavelet transform of Eq. (2) would be:

$$y_\ell = f_\ell + n_\ell \tag{3}$$

where y_ℓ, f_ℓ and n_ℓ represent noisy and noise free data and AWGN in wavelet transform respectively.

B. Thresholding Rules

Sparsity that means most coefficients are approximately zero, plays a key role in any thresholding algorithms. The sparsity is a typical characteristic of wavelet domain where noise is uniformly spread through all coefficients and the data is represented by a small subset of big coefficients [16]. So, coefficients with small magnitude can be considered as noise and set to zero. The approach in which each coefficient is compared with a threshold in order to decide whether it constitute a desired part of the original data or not is called thresholding. As a matter of facts, the main assumption that indicates the validity of thresholding is the sparsity of coefficients. Whereas sparsity is directly related to the choice of a basis, the Gaussian noise representation is not sparse in any given basis [22]. To support the idea, Fig. 2 shows the histogram of clean and noisy coefficients for three detail sub-bands of first decomposition level of DWT. As seen in Fig. 2, existing noise decreases the signal sparsity and also adds some undesired nonzero coefficients. Using thresholding rules, these coefficients are set to zero.

There are four well-known thresholding rules named as hard [5], soft [26], Exp. [16] and Garrote [15], [27]. As a matter of fact, detail coefficients of noisy data y_ℓ in wavelet transform are used to compute the threshold value at each decomposition level and thresholding is applied to all detail coefficients, including: horizontal h_ℓ, vertical v_ℓ and diagonal d_ℓ coefficients. The corresponding equations are given in following and shown in part in Fig. 1,

$$\delta_\lambda^{Hard}(y_\ell) = \begin{cases} 0 & , \ |d_\ell| \le \lambda \\ d_\ell & , \ |d_\ell| > \lambda \end{cases} \tag{4}$$

$$\delta_\lambda^{Soft}(y_\ell) = \begin{cases} 0 & , \ |d_\ell| < \lambda \\ \operatorname{sgn}(d_\ell)(|d_\ell| - \lambda) & , \ |d_\ell| > \lambda \end{cases} \tag{5}$$

$$\delta_\lambda^{Exp}(y_\ell) = \begin{cases} d_\ell \, e^{p_\ell(|d_\ell| - \lambda)} & , \ |d_\ell| < \lambda \\ d_\ell & , \ |d_\ell| \ge \lambda \end{cases} \tag{6}$$

$$\delta_\lambda^{Garrote}(y_\ell) = \begin{cases} 0 & , \ |d_\ell| \le \lambda \\ d_\ell - \dfrac{\lambda^2}{d_\ell} & , \ |d_\ell| > \lambda \end{cases} \tag{7}$$

where λ is the threshold value; y_ℓ refers to noisy detail sub-band, including h_ℓ, v_ℓ, d_ℓ; $\delta_\lambda(.)$ is the output denoised coefficient; $\operatorname{sgn}(.)$ is the signum function and p_ℓ in Eq. (6) is the fall degree of exponential function for $\ell - th$ decomposition level which the optimized value was introduced in [16].

In contrast with hard thresholding that preserves the coefficients greater than the threshold value, soft thresholding shrinks the coefficients and because of that, it yields bias estimates [15]. Therefore, hard thresholding produces less biased but higher variance estimates and it may be unstable due to discontinuous nature. In other words, discontinuity of hard thresholding can lose data and diminish edge preservation. To avoid both hard and soft thresholding drawbacks, the Exp. thresholding, Eq. (6), is able to gradually reduce the coefficients in the zero zone and the "non-negative Garrote" function, Eq. (7), is one of the represented ad-hoc rules [27].

C. Estimating Noise Power

Finding the optimal value λ is an important issue for any thresholding method. However, the first step for this purpose is noise power estimation. Median absolute deviation [19], Quantile median [28] and Marginal variance [29] were proposed for this purpose. Although there are three detail coefficients, only diagonal coefficients d_ℓ are used for computing the noise power.

C.1. Median Absolute Deviation

A popular estimate of noise standard deviation at $\ell - th$ level is based on the diagonal detail coefficients [19].

$$\hat{\sigma}_n = \frac{\text{median}\left(|\, d_\ell \,|\right)}{0.6745} \tag{8}$$

Eq. (8) is based on two assumptions, the first is considering the noise n_ℓ an independent Gaussian random variable of zero mean and variance $\hat{\sigma}_n^2$ at each level, and the second is considering that the signal has sparse representation in wavelet domain, so that most wavelet coefficients are just noise.

C.2. Quantile Median

Mathematics uses a slightly different form of Eq. (8) for the noise estimation [28],

$$\hat{\sigma}_n = \frac{\text{median}\left(|\, d_\ell \,|\right)}{\text{Quantile}\left[\text{Normal Distribution}\ (n_\ell), \frac{3}{4}\right]} \tag{9}$$

where the Quantile refers to cut points dividing the range of a probability distribution into continuous intervals with equal probabilities. So, the denominator refers to the third quartile of n_ℓ, which is a type of Quantile . The quartiles of a ranked set of data values are the three points that divide the data set into four equal groups, each group comprising a quarter of the data. In fact, quartiles are the three cut points that will divide a dataset into four equal-size groups. The first quartile is defined as the middle number between the smallest number and the median of the data set, the second quartile is the median of the data and the third quartile is the middle value between the median and the highest value of the data set. The difference between the constant 0.6745 and the ¾ quartile of the normal distribution is 1.02498×10^{-5} or a relative difference of 0.0015%.

C.3. Marginal Variance

According to the Marginal variance method [29], the noise standard deviation $\hat{\sigma}_n$ at $\ell - th$ level is,

$$\hat{\sigma}_n = \sqrt{\sigma_y^2 - \sigma_\ell^2} \tag{10}$$

where σ_ℓ is obtained by Eq. (8), $\sigma_y^2 = (1/S)\times \sum_{y_\ell \in Y} y_\ell^2$ is the Marginal variance and *S* is the size of picture. In fact, y_ℓ and $y_{\ell+1}$ are noisy versions of noise-free coefficients f_ℓ and $f_{\ell+1}$ where $f_{\ell+1}$ is the coefficient at the same position as f_ℓ , but at the next coarser scale.

III. Threshold Based Denoising Methods

The choice of a threshold value is a crucial phase for the wavelet threshold based methods. In fact, the threshold separates the undesired coefficients corresponding to the noise and the significant coefficients useful to recover the data. A low threshold value preserves the details but does not reduce the noise sufficiently while a large threshold value reduces the noise but may destroy the details [16]. In order to balance the side effects, different thresholding techniques were proposed. Each method, considering the noise power $\hat{\sigma}_n$, uses its own procedure to compute the threshold value λ.

A. VisuShrink

This method takes into account only the image size *S* and the noise standard deviation $\hat{\sigma}_n$ in order to obtain the universal threshold for all sub-bands [30]:

$$\lambda^{Universal} = \hat{\sigma}_n^2 \sqrt{2 \log S} \tag{11}$$

B. SureShrink

This method computes the threshold values for each sub-band,

$$\lambda^{\text{SureShrink}} = \begin{cases} \lambda^{Universal}, & \text{if} \quad Q_S(d_i) \le 1 \\ \lambda^{*}, & \text{otherwise} \end{cases} \tag{12}$$

where $Q_S(d_i) = \left(S^{-1/2}\sum_{i=1}^{S}(d_i^2 - 1)\right) \Big/ \log_2^{3/2}(S)$ is a measure of sparsity for coefficients [5], $\lambda^* = \underset{0\le\lambda<\lambda^{Universal}}{\arg\min}\ SURE(\lambda, d)$ is the optimal threshold which denotes the value that minimizes the SURE function, $SURE(\lambda, d) = S + \sum_{i=1}^{S}\left[\min\left(|\, d_i \,|, \lambda\right)\right]^2 - 2$ where i should satisfy $|d_i| < \lambda^{Universal}$.

C. NeighBlock

The NeighBlock threshold [31] value is,

$$\lambda^{NeighBlock} = \frac{S_{\ell B}^2 - \lambda_C L}{S_{\ell B}^2} \tag{13}$$

where $S_{\ell B}^2$ denotes the energy of each analyzing block (sum of squared coefficients), L is the block size and $\lambda_C = 4.505$ according to [32]. In fact, the wavelet coefficients are grouped into disjoint blocks (ℓb) of length $L_0 = \left\lfloor \frac{\log S}{2} \right\rfloor$ and each block is extended by an amount of $L_1 = \max\left(1, \lfloor L_0/2 \rfloor\right)$ in every direction. So, overlapping blocks (ℓB) of length $L = L_0 + 2L_1$ are formed. The threshold value in each block (ℓb) is estimated according to Eq. (13).

The basic motivation of working with blocks is that if neighboring coefficients contain important part of the signal, then it is likely that the current coefficient is also important and so lower threshold is to be used. This yields a local tradeoff between data and noise. Besides, this method

increases the estimation precision by utilizing information about neighboring wavelet coefficients. The threshold level is chosen per group (blocks) of coefficients according to their local properties, where each group contains a subset of the coefficients in the current resolution level.

IV. EXPERIMENTAL RESULTS

In this section, for Barbara test image with size 256×256 and 256 gray levels, the performance of denoising algorithms are evaluated. For this purpose, hard, soft, Exp. and Garrot as thresholding rules; VisuShrink, SureShrink and NeighBlock as thresholding methods; and Median absolute deviation, Quantile Median and Marginal variance as noise power estimators are used. Fig. 1 shows the block diagram.

In order to compare the three introduced noise power estimators, we have used a flat gray image (i.e. the gray level of all pixels is 128 and so the image variance intensity is zero) with size 256×256. The image is corrupted by noise of variances 0.1, 0.3 and 0.5. Then the noise power of different levels in wavelet transform are estimated by using Median absolute deviation, Quantile median and Marginal variance. As seen in Fig. 3, while the Median absolute deviation estimates the noise power values accurately for all seven decomposition levels, Quantile median and Marginal variance experience inconsistency after the sixth decomposition level. Moreover, Quantile median has a bias for low power noise but it estimates the high power noise precisely.

In this paper, an input image is decomposed into five levels by DWT where "db4" as the wavelet is used. For Barbara as a sample test image, the results are shown in Figs. 4 - 6, where the speckle noise variance is 0.3. As seen in Fig. 4 for VisuShrink thresholding method, there is a trade-off between denoising and detail preserving. Whereas in Fig. 5 for SureShrink thresholding method, the bottleneck is being images blur and seeing artifact. In contrast, for NeighBlock thresholding method as shown in Fig. 6, the images edges are preserved but still remaining the noise.

As a matter of fact, detail detection is the most important factor which affect our eyes when they are choosing the best image. That is to say, regardless of the residual noise, our eyes prefer the images that their edges and details are more preserved. So, the SureShrink under using different noise power estimators and thresholding rules is not appropriate in comparison with VisuShrink in part and NeighBlock. However, visual evaluation and image assessment parameters may not agree in conclusion. Therefore, in this paper, three well-known image criteria are used, consisting: PSNR [16] which measures the image quality, SSIM [33] that predicts the perceived quality of picture, and β [16] which measures the edge preservation. Results of traditional quality indexes are written in Table 1 for sample image "Barbara" under the noise variance 0.3. As the values written in Table 1 indicates, there is a tradeoff between denoising and edge preservation.

According to the limitations and characteristics of each method and our results, it can be concluded that the performance of VisuSrink with Garrot thresholding rule and Median absolute deviation noise power estimator is appropriate in comparison with other methods, noise estimators, and thresholding rules.

V. CONCLUSION

In this paper, the wavelet based denoising methods for despeckling were compared and the best algorithm was proposed by focusing on the role of noise power estimators and the influence of thresholding rules. Owing to the fact that there is a tradeoff between denoising and edge preservation, the best output should be determined based on the user's desires. But in this paper we tried to propose the most optimal method as a package by comparing the output images and image assessment parameters precisely. To put in a nut shell, the most optimal package for despeckling in wavelet domain is introduced as using Garrot thresholding rule and Median absolute deviation in VisuSrink denoising method. In further studies, our research would be channeled to covering the mentioned tradeoff by analyzing and comparing more denoising methods.

REFERENCES

[1] I.M. Johnstone, "Wavelets and the theory of nonparametric function estimation," Philosophical Transactions of the Royal Society London Ser. A 357, pp. 2475–2493, 1999.

[2] R. F. Wagner, S. W. Smith, J. M. Sandrick, and H. Lopez, "Statistics of speckle in ultrasound B-scans," IEEE Transaction on Sonics Ultrasonics, vol. 30, no. 3, pp. 156–163, May 1983.

[3] Alessandro Foi, Mejdi Trimeche, Vladimir Katkovnik, and Karen Egiazarian." Practical Poissonian-Gaussian noise modeling and fitting for single image raw-data," IEEE Transactions on Image Processing, No. 17, pp. 1737-1754, 2008.

[4] Wiener, Extrapolation, Interpolation, and Smoothing of Stationary Time Series, Wiley, New York, NY, 1949.

[5] David L. Donoho and Iain M. Johnstone. "Adapting to unknown smoothness via wavelet shrinkage," Journal of the American Statistical Association, pages 1200-1224, 1995.

[6] T. Loupas, W. Mcdicken, and P. Allen, "An adaptive weighted median filter for speckle suppression in medical ultrasound images," IEEE Transaction on Circuit System, vol. 36, no. 1, pp. 129–135, Jan. 1989.

[7] Y. Chena, R. Yinb, P. Flynn, and S. Broschatd, "Aggressive region growing for speckle reduction in ultrasound images," Pattern Recognition Letter, vol. 24, no. 4–5, pp. 677–691, Feb. 2003.

[8] J. I. Koo and S. B. Park, "Speckle reduction with edge preservation in medical ultrasonic images using a homogeneous region growing mean filter (HRGMF)," Ultrasonic Imaging, vol. 13, no. 3, pp. 211–237, Jul. 1991.

[9] F. Jin, P. Fieguth, L. Winger, and E. Jerniga, "Adaptive Wiener filtering of noisy images and image sequences," International Conference on Image Processing, pp. 349–352, Sep. 2003.

[10] D. Hillery and R. T. Chin, "Iterative Wiener filters for images restoration," IEEE Transaction on Signal Processing, vol. 39, no. 8, pp. 1892–1899, Aug. 1991.

[11] S. Mallat, "A Wavelet Tour of Signal Processing," Academic Press, San Diego, 1998.

[12] M. Steinbuch and M.J.G. van de Molengraft. "Wavelet theory and applications: A literature study," Technical report, Eindhoven University of Technology, 2005.

[13] S.G. Mallat. "A theory for multiresolution signal decomposition: the wavelet representation," IEEE Transactions on Pattern Analysis and Machine Intelligence," No. 11, pp. 674-693, July 1989.

[14] S. Tsai. "Wavelet transform and denoising. Master's thesis," Chapter 4, pp. 35-42, 2002.

[15] Mário A. T. Figueiredo and Robert D. Nowak, "Wavelet-Based ImageEstimation:An Empirical Bayes ApproachUsing Jeffreys' Noninformative Prior," IEEE Transaction on Image Proscessing, vol. 10, no. 9, Sept. 2001.

[16] Gregorio Andria, Filippo Attivissimo, Anna M. L. Lanzolla, and Mario Savino, "A Suitable Threshold for Speckle Reduction in Ultrasound Images," IEEE Transaction on Instrumentation and Measurement, vol. 62, no. 8, Agust 2013.
[17] L. Mateo and A. Fern´andez-Caballero, "Finding out general tendencies in speckle noise reduction in ultrasound images," Expert System, vol. 36, no. 4, pp. 7786–7797, May 2009.
[18] David L. Donoho and Iain M. Johnstone. "Minimax estimation via wavelet shrinkage,"
Technical report, 1992.
[19] David L. Donoho and Jain M. Johnstone."Ideal spatial adaptation by wavelet shrinkage," Biometrika, 81(3):425-455, 1994.
[20] C. B. Burckhardt, "Speckle in ultrasound B-mode scans," IEEE Transaction on Sonics Ultrasonics, vol. 25, no. 1, pp. 1–6, Jan. 1978.
[21] M. Ghazel, G. H. Freeman, E. R. Vrscay, and R. K. Ward, "Wavelet image denoising using localized thresholding operators," Image Annals Recognition, vol. 36, no. 56, pp. 149–158, Nov. 2005.
[22] Albert C.To, JeffreyR.Moore, StevenD.Glaser, "Wavelet denoising techniques with applications to experimental geophysical data," Signal Processing, no. 89, pp. 144–160, 2009.
[23] S. Gupta, R. C. Chauhan, and S. C. Sexana, "Wavelet-based statistical approach for speckle reduction in medical ultrasound images," Medical and Biological Engineering and Computing, vol. 42, no. 2, pp. 189–192, Feb. 2004.
[24] P. M. Shankar "A general statistical model for ultrasonic backscatterin from tissues," IEEE Transaction on Ultrasonics, Ferroelectrics and Frequency Control, vol. 47, no. 7, pp. 727–736, Jun. 2000.
[25] M. Jansen and A. Bulthool, "Multiple wavelet threshold estimation by generalized cross validation for images with correlated noise," IEEE Transaction on Image Processing, vol. 8, no. 5, pp. 947–953, Jun. 1999.
[26] David L. Donoho. "Denoising by soft-thresholding," IEEE Transaction on Information
Theory, no. 41, pp. 613-627, May 1995.
[27] H. Gao, "Wavelet shrinkage denoising using the nonnegative garrote," Journal of Computational and Graphical Statistics, vol. 7, pp. 469–488, 1998.
[28] Rob J. Hyndman and Yanan Fan "Sample Quantiles in Statistical Packages," The American Statistician, vol. 50, No. 4, pp. 361-365, Nov. 1996.
[29] Fei Gao, Xiangshang Xue and Jinping Sun,"A SAR Image Despeckling Method Based on Two-Dimensional S Transform Shrinkage," IEEE Transaction on Geoscience and Remote Sensing ,Vol. 54, no. 5, May 2016.
[30] A. Achim, A. Bezerianos, and P. Tsakalides, "Novel bayesian multiscale method for speckle removal in medical ultrasound images," IEEE Transaction on Medical Imaging, vol. 20, no. 8, pp. 772–783, Aug. 2001.
[31] T.T. Cai and B.W. Silverman. "Incorporating information on neighbouring coe_cients into wavelet estimation," Sankhya, Series A, 63, 2001.
[32] T. Tony Cai, Keywords James-stein, "Estimator Adaptivity, Wavelet Block, and Thresholding Nonparametric. Adaptive wavelet estimation: A block thresholding and oracle inequality approach," The Annals of Statistics, no. 27, pp. 898-924, 1998.
[33] Z. Wang, A.C. Bovik, H.R. Sheikh, E.P. Simoncelli, "Image quality assessment: from error visibility to structural similarity," IEEE
Transactions on Image Processing, Vol. 13, No. 4, pp. 600–612, April 2004.

Alireza Mohammad Zaki recieved B.Sc. degree in Electronic Engineering from Islamic Azad University – South Tehran Branch in 2017. His interest is Signal and image processing. He wishes to continue his graduate studies in Mixed Signal Processing.

Sedigheh Ghofrani received BSc degree in Electronic Engineering from Tehran University in 1991, the MSc. degree in communication from Islamic Azad University, south Tehran branch in 1997 and Ph.D in Electronic from Iran university of Science and Technology in 2004. She has been the assistant professor of Electronic and Electrical Engineering Department at the Islamic Azad University, south Tehran branch from 2004 to 2011 and associate professor since 2012. Her area of research includes image processing and signal processing.

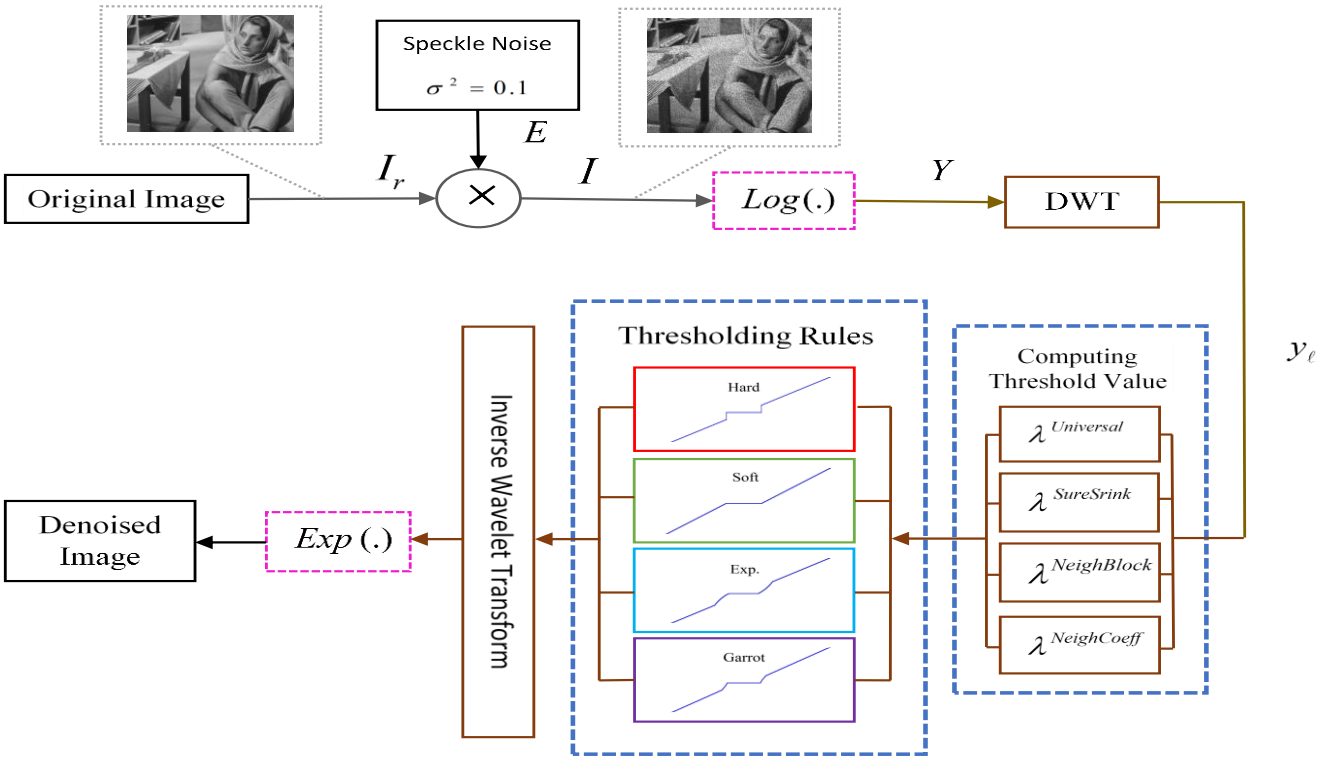

Fig. 1. The block diagram of speckle denoising in DWT domain.

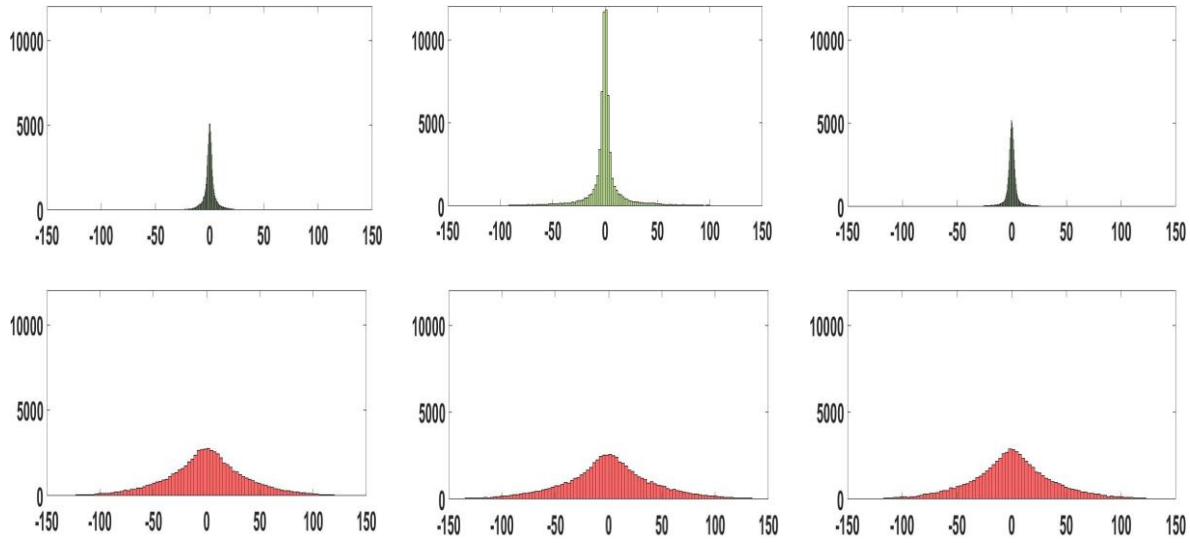

Fig. 2. Histogram of first-level wavelet detail coefficients, h_1 (first column), v_1 (second column), d_1 (third column), for clean data (first row) and noisy data (second row) where the noise power is 0.1.

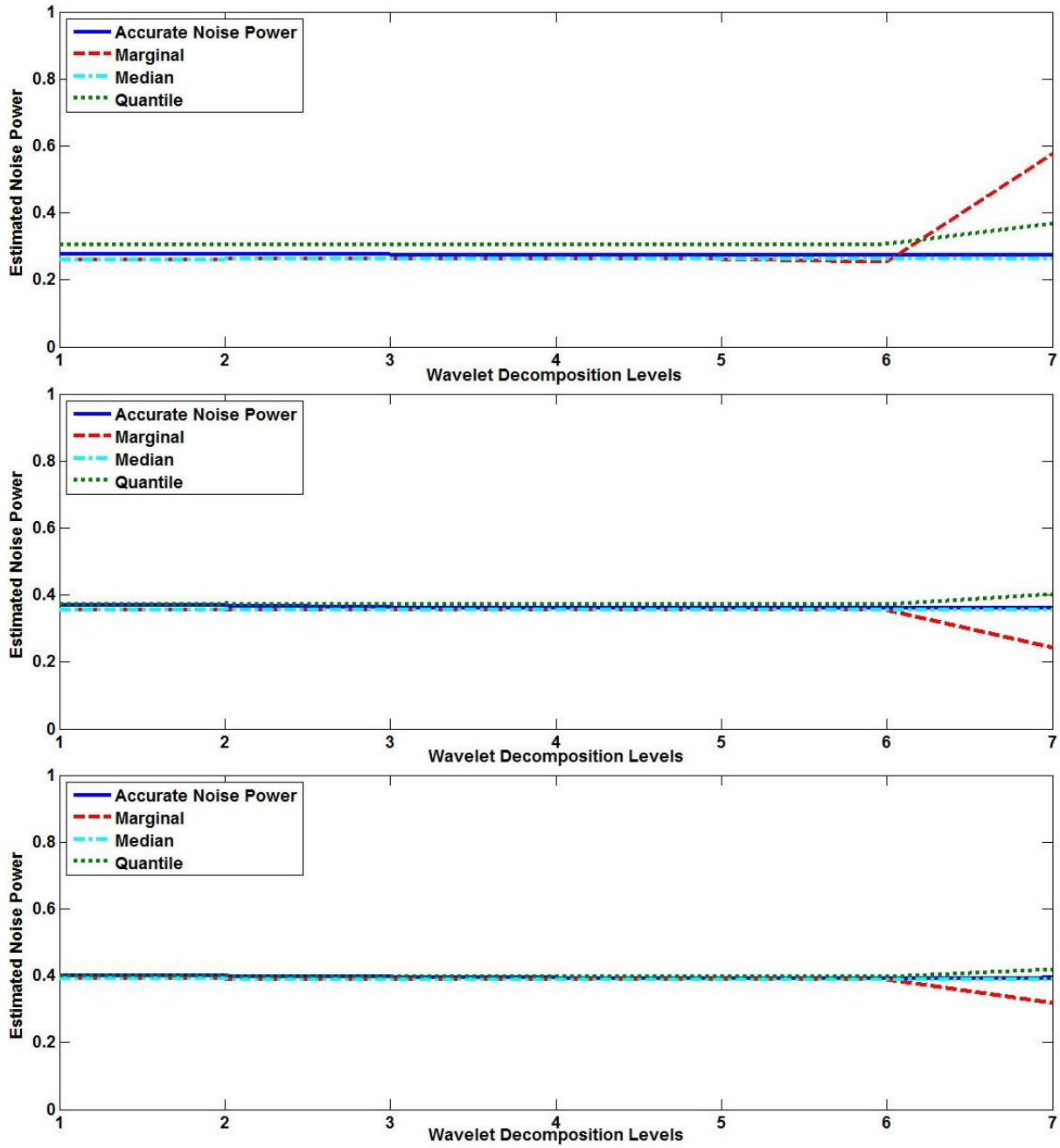

Fig. 3. Output of three proposed methods for estimating the noise power of 1 to 7 wavelet decomposition levels for flat Gray image where the noise variance is 0.1, 0.3 and 0.5, respectively.

Fig. 4. Results of VisuShrink thresholding method for denoising Barbara by using Median absolute deviation (first row), Quantile median (second row), Marginal variance (third row) for noise power estimation and Hard (first column), Soft (second column), Exp. (third column), Garrot (forth column) as the thresholding rule under noise variance 0.3.

Fig. 5. Results of SureShrink thresholding method for denoising Barbara by using Median absolute deviation (first row), Quantile median (second row), Marginal variance (third row) for noise power estimation and Hard (first column), Soft (second column), Exp. (third column), Garrot (forth column) as the thresholding rule under noise variance 0.3.

Fig. 6. Results of NeighBlock thresholding method for denoising Barbara by using Median absolute deviation (first row), Quantile median (second row), Marginal variance (third row) for noise power estimation and Hard (first column), Soft (second column), Exp. (third column), Garrot (forth column) as the thresholding rule under noise variance 0.3.

Table 1. Traditional quality indexes of proposed denoising methods when image is contaminated by noise variance 0.3.

		PSNR				SSIM				B ($\times 10^{-4}$)			
		Hard	**Soft**	**Exp.**	**Garrot**	**Hard**	**Soft**	**Exp.**	**Garrot**	**Hard**	**Soft**	**Exp.**	**Garrot**
VisuShrink	**Median**	18.36	20.03	18.34	**20.33**	0.38	0.47	0.38	0.46	1.43	1.36	**1.44**	1.36
	Quantile	19.96	19.65	19.96	20.08	0.45	0.47	0.45	**0.48**	1.43	1.37	1.43	1.37
	Marginal	18.41	20.05	18.40	20.32	0.38	0.47	0.38	0.46	1.36	1.36	1.36	1.35
SureShrink	**Median**	20.04	19.19	20.05	19.57	0.47	0.46	0.47	0.46	1.34	1.36	1.34	1.35
	Quantile	**20.29**	19.48	**20.29**	19.92	**0.48**	0.47	**0.48**	**0.48**	1.35	**1.37**	1.35	1.35
	Marginal	20.10	19.21	20.10	19.60	**0.48**	0.46	**0.48**	0.47	1.33	1.36	1.33	1.34
NeighBlock	**Median**	12.90	17.52	12.88	15.37	0.23	0.35	0.23	0.31	1.84	1.74	**1.85**	1.80
	Quantile	13.35	**18.44**	13.33	16.45	0.25	**0.37**	0.25	0.33	1.80	1.65	1.81	1.73
	Marginal	12.85	17.41	12.84	15.24	0.23	0.35	0.23	0.30	1.84	1.75	**1.85**	1.81